CHAPTER SIX

PHYSICAL AND MECHANICAL PROPERTIES OF PI/TiO$_2$ NANO

HYBRID FILMS

Summary

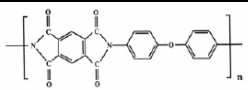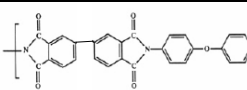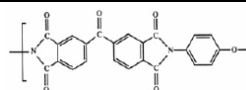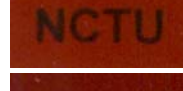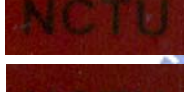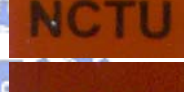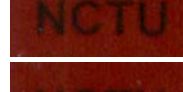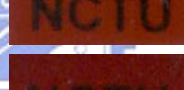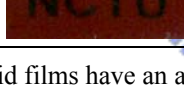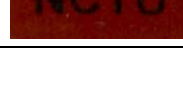The demand for materials with novel combination of properties has led to the recent efforts in modification of known polymers via the incorporation of a variety of additives. In this study, three kinds of polyimide (PI) systems are chosen as the matrices and incorporated with titania (TiO$_2$) in the range of 1 wt% to 9 wt%. These hybrid films are based on 4,4'-diaminodiphenylether (ODA) and various dianhydrides. The work presented here attempts to investigate the structure-property relationship and the effect of TiO$_2$ content upon thermal, mechanical, and electrical properties of PI/TiO$_2$ hybrid films.

6.1 PI/TiO$_2$ Hybrid Films Appearance

The polyimides chosen in this study have structures depicted in Table 6.1. During the preparation of the hybrid films, all the poly(amic acid)/titanium alkoxide mixtures remain homogeneous and transparent. Upon curing to the fully imidized polymer, PMDA/ODA, BPDA/ODA, and BTDA/ODA form transparent, flexible, free-standing and golden-yellow films. In the cases of TiO$_2$ incorporated, the hybrid films with homogeneous and brown color are obtained. Table 6.1 presents the films that are synthesized and characterized in this study. It can be seen that the more TiO$_2$ is contained, the less flexibility and deeper color are showed for the hybrid films. All the hybrid films are less transparent than host polyimides. From TEM observation (Figure 6.1), the particle size of TiO$_2$ is about 25 nm for BTDA/ODA-TiO$_2$ 9 wt% hybrid film. In the series of PMDA/ODA, the hybrid films containing TiO$_2$ of 5 wt% or more are brittle. While the series of

BPDA/ODA and BTDA/ODA based hybrid films are still flexible with TiO$_2$ content up to 5 wt% or more. This result indicates that the flexibility of PI/TiO$_2$ hybrid films has an order of BTDA/ODA > BPDA/ODA > PMDA/ODA.

Table 6.1 Chemical structures of PI and PI/TiO$_2$ hybrid films appearance.

TiO$_2$ Content	PMDA/ODA	BPDA/ODA	BTDA/ODA
0 wt%	NCTU	NCTU	NCTU
1 wt%	NCTU	NCTU	NCTU
3 wt%	NCTU	NCTU	NCTU
5 wt%	NCTU	NCTU	NCTU
7 wt%	NCTU	NCTU	NCTU
9 wt%	NCTU	NCTU	NCTU

[a] The PI/TiO$_2$ hybrid films have an average final thickness of 35 ~ 40 μm.
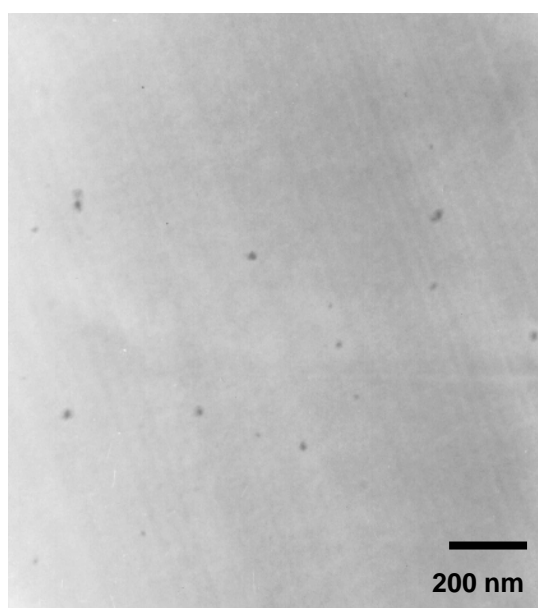
Figure 6.1 TEM photograph of BTDA/ODA-TiO$_2$ 9 wt% hybrid film.

60

6.2 Coefficients of Thermal Expansion (CTE) Analysis

From the data in Table 6.2, there is a marked reduction of thermal expansion for the PI/TiO$_2$ hybrid films. This dramatic decrease in CTE could be due to metals and inorganic materials (TiO$_2$) having lower CTE values. Besides, the network structure of TiO$_2$ domains could lead to decrease the segmental mobility of the polyimide chains [1-4]. That is why the lower values of CTE for the PI/TiO$_2$ hybrid films are obtained.

In Table 6.2, the CTE of PI/TiO$_2$ hybrid films are measured in the range of 50-200℃. For all these hybrid films, there is a similar tendency of decreasing CTE with increasing TiO$_2$ content as shown in Figures 6.2 to 6.4. Besides, the decrease of CTE values at elevated temperature is more remarkable. This property will enhance the reliability for applications at high temperature. It is also interesting to note that the PMDA/ODA based hybrid films have much lower CTE values as compared with the other two series at elevated temperature. This could be resulted from the PMDA/ODA possessing higher glass transition temperature (T_g) than BPDA/ODA and BTDA/ODA. Thus, the increase of CTE for the latter two series could be due to the rise of chain mobility at the temperature close to their T_gs.

Table 6.2 Coefficients of thermal expansion (CTE) of PI/TiO$_2$ hybrid films.

TiO$_2$ Content	CTE (ppm/K)[a]		
	PMDA/ODA	BPDA/ODA	BTDA/ODA
0 wt%	32.5	43.4	45.6
1 wt%	27.9	37.8	42.6
3 wt%	20.2	28.6	38.3
5 wt%	17.3	24.7	33.7
7 wt%	[b]	21.0	29.3
9 wt%	[b]	[b]	26.1

[a] The CTE of PI/TiO$_2$ hybrid films are determined over a range of 50-200℃.
[b] The hybrid film is too brittle and fragile to obtain satisfactory for measurement.
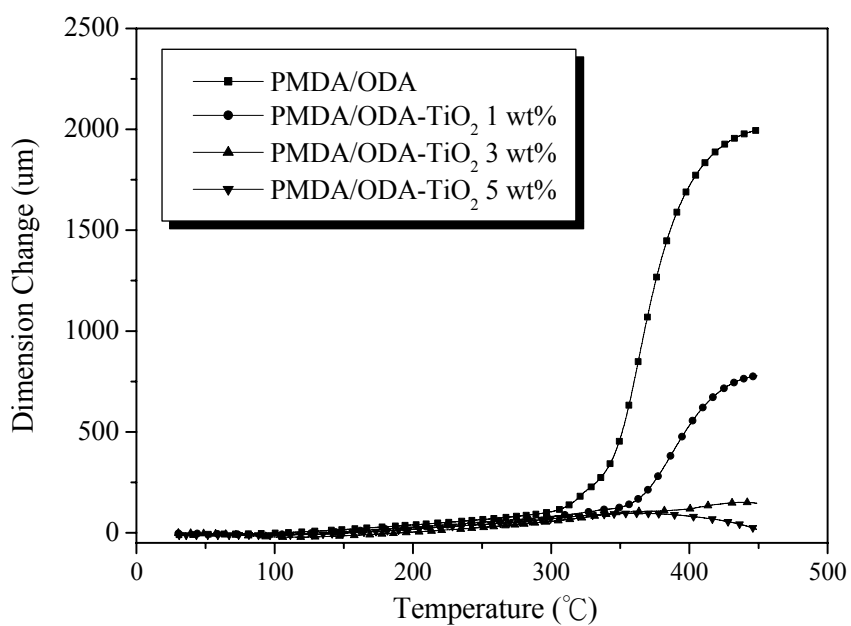
Figure 6.2 Thermal expansion of PMDA/ODA-TiO$_2$ hybrid films.
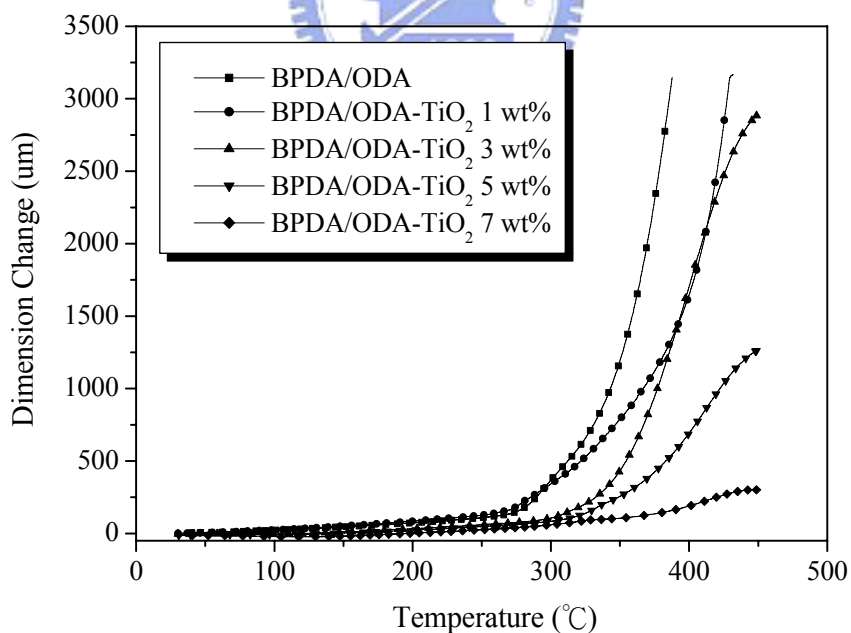
Figure 6.3 Thermal expansion of BPDA/ODA-TiO$_2$ hybrid films.
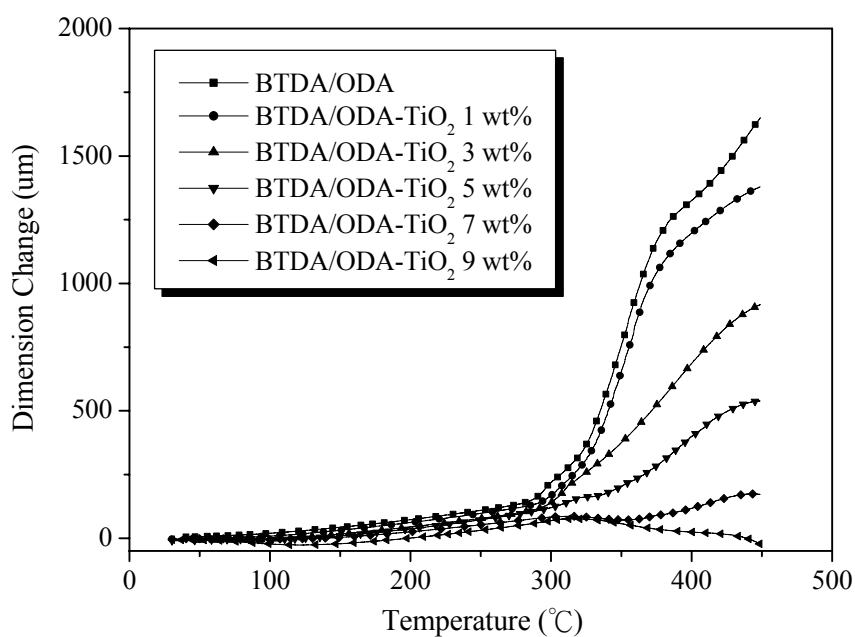
Figure 6.4 Thermal expansion of BTDA/ODA-TiO$_2$ hybrid films.
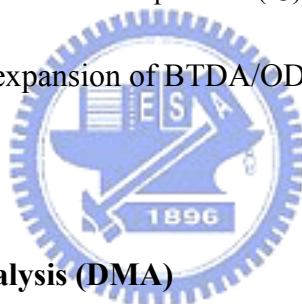
6.3 Dynamic Mechanical Analysis (DMA)

Figures 6.5-6.7 show the storage modulus (E'), loss modulus (E'') and tan δ as a function of temperature for the various PI/TiO$_2$ hybrid films. For each series of PI/TiO$_2$ hybrid films, the storage modulus decreases with increasing the temperature, but increases slightly around their T_gs. It is suggested that additional cross-linking occurs at these elevated temperatures due to further inorganic condensation reaction and covalent bonding with the polyimide [5-7]. Moreover, the loss modulus curve displays two distinct transitions at 65-100℃ and 300-350℃ in the entire range. The low-temperature one is associated with local bond rotations and molecular segment motions along the polymer backbone and defined as the β-relaxation or subglass transition. The high-temperature one, defined as the α-relaxation or primary glass transition, is attributed to the motion of polyimide backbone [8-10].
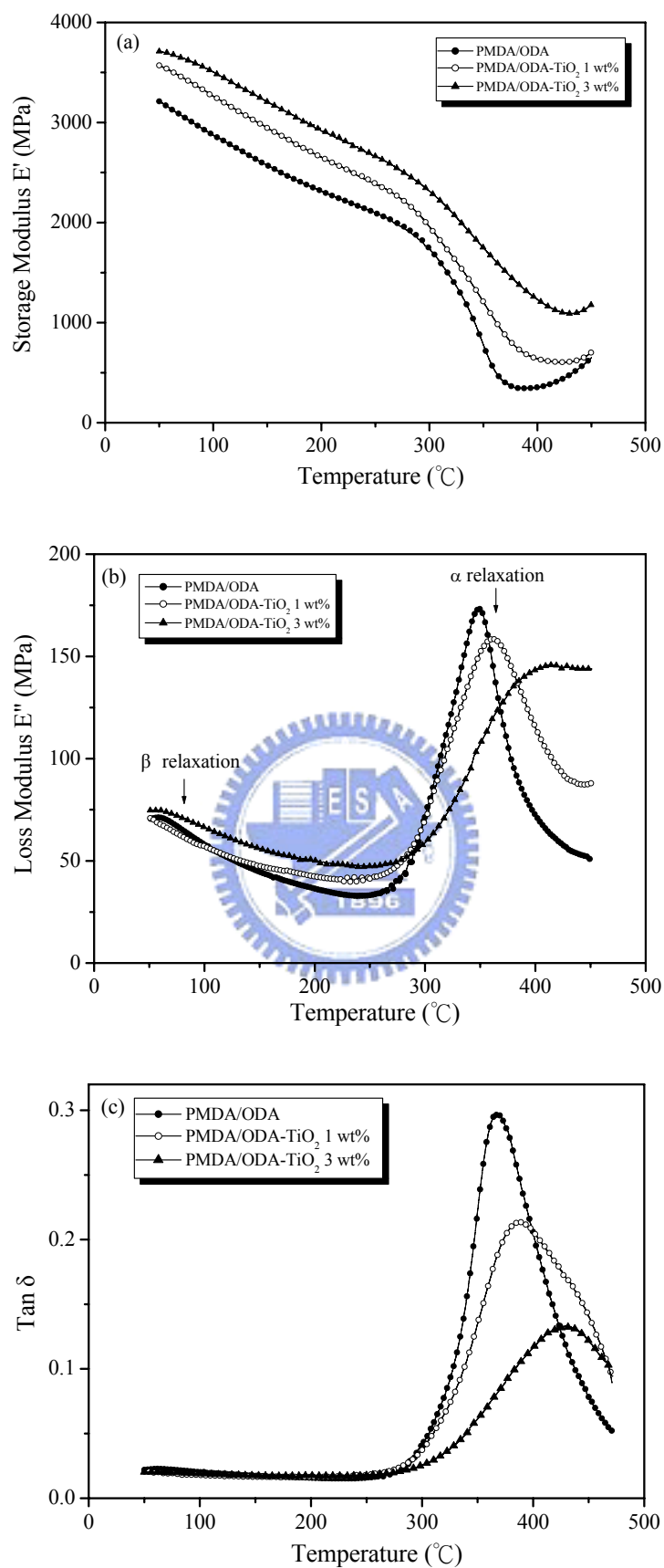
Figure 6.5 (a) the storage modulus, (b) the loss modulus and (c) the tan δ curves of PMDA/ODA-TiO₂ hybrid films at different temperatures.
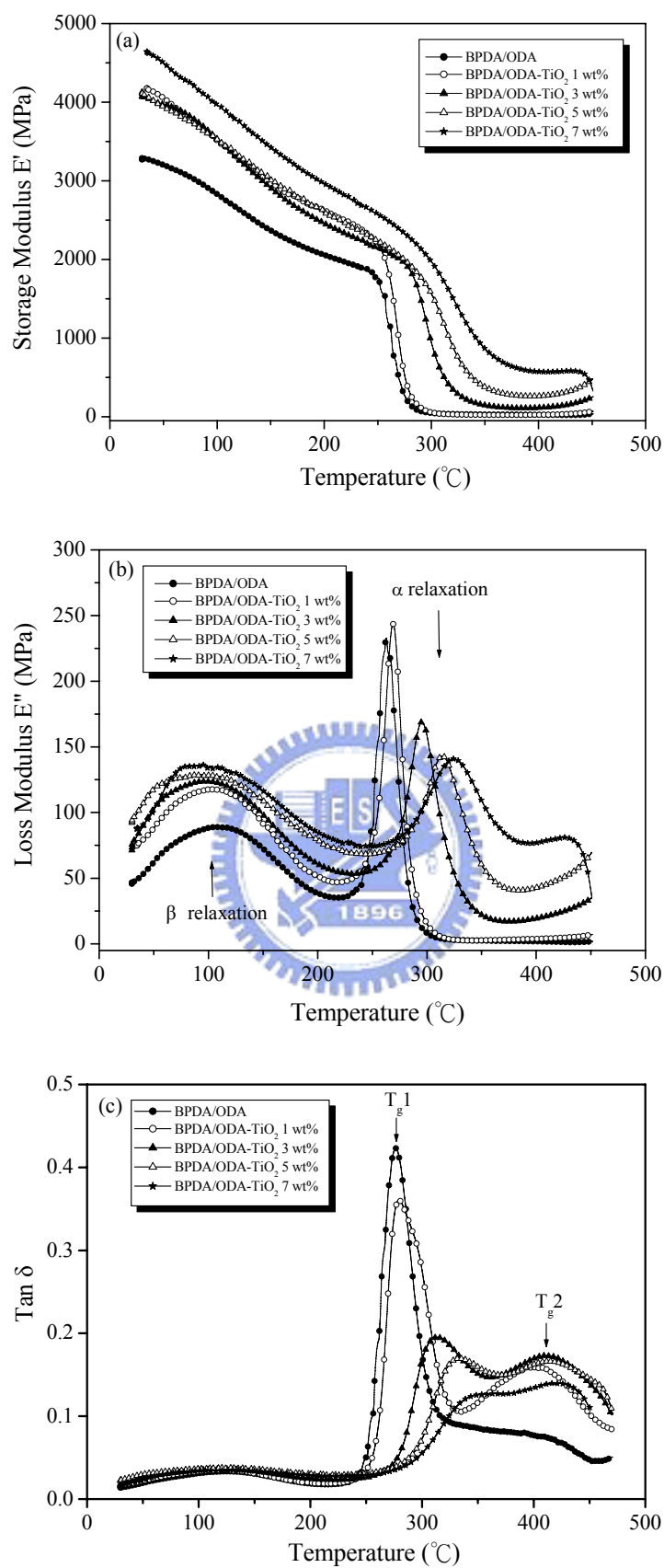
Figure 6.6 (a) the storage modulus, (b) the loss modulus and (c) the tan δ curves of BPDA/ODA-TiO$_2$ hybrid films at different temperatures.
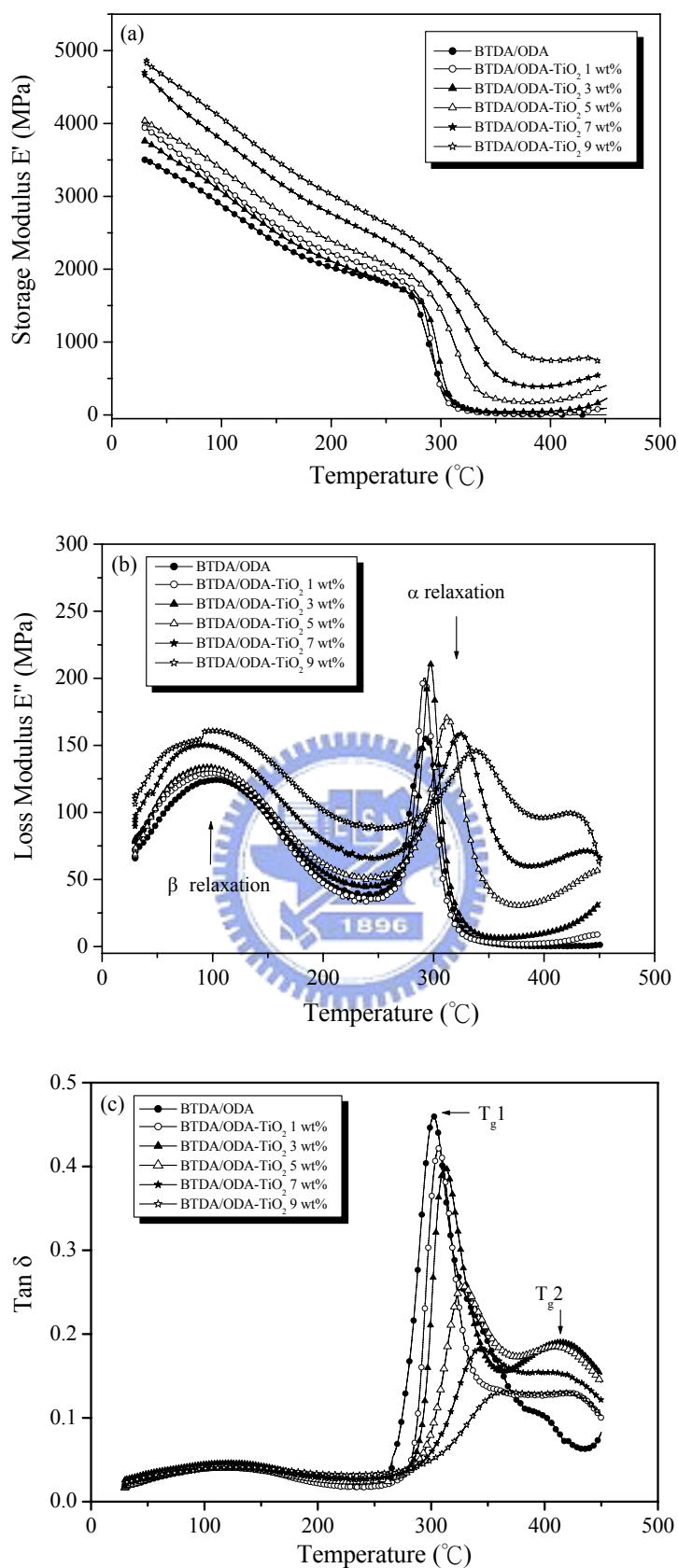
Figure 6.7 (a) the storage modulus, (b) the loss modulus and (c) the tan δ curves of BTDA/ODA-TiO$_2$ hybrid films at different temperatures.

The correlation between TiO_2 content and storage/loss modulus also can be seen in Figures 6.5-6.7. As the TiO_2 content in the hybrid films increases, the value of the storage modulus becomes larger and the magnitude of loss modulus at T_g is reduced. The increase of storage modulus is ascribed to the incorporation of TiO_2 forming network structure and increasing the rigidity of the hybrid films [1, 2, 11-13]. With regard to the loss modulus, the cross-linked structure of hybrid films makes the lower interaction force between molecular chains. Therefore, the lower loss modulus at T_g is obtained for the PI/TiO_2 hybrid films.

For all the PI/TiO_2 hybrid films, the glass transition temperature, T_g, is taken at the maximum tan δ (E''/E'). According to Figures 6.5-6.7, these results are summarized in Table 6.3. Each hybrid film shows higher T_g as compared with the host polyimide. In general, the T_g of the hybrid films increases with increasing TiO_2 content. This increase may be due to the filler effect of the TiO_2, thereby affording more stiff hybrid films. Besides, the cross-linking reactions between polyimide and titanium ethoxide would be expected to increase T_g [14-16].

The content of TiO_2 also has an effect on the cooperative motions of polymer chains at T_g. The magnitude of tan δ at T_g is a measure of energy-damping characteristic of a material and the breadth of the tan δ relaxation is indicative of the cooperative nature of the relaxation process of the polymer chains [17-19]. Conceptually, cooperative can be related to the ease at which polymer chains move in concert through the glass transition, while non-cooperative materials have polymer chains that resist concerted motion that are characterized by very broad tan δ peak.

In this study, the magnitude of tan δ decreases with increasing the TiO_2 content for the hybrid films. This is a result of the increase of rigidity and the cross-linked structure

of the hybrid films. On the other hand, the breadth of the tan δ through the T_g is characterized by small to very significant broadening and additional transitions above the T_g are observed for both BPDA/ODA and BTDA/ODA series.

For PMDA/ODA based hybrid films, there is an increasing tan δ breadth with increasing TiO$_2$ content. Whereas, for BPDA/ODA and BTDA/ODA based hybrid films, there is not only broadening of tan δ, but an additional transition at higher temperature is observed, which is indicative of another molecular transition [20-23]. The new tan δ around 400-420℃, defined as T_g2, suggests the presence of an inorganic/organic phase, which may have a higher T_g as compared with the polyimide. It may also be a consequence of additional inorganic condensations and cross-linking reactions with the polyimide matrix which are taking place at higher DMA testing temperatures. The shifts of T_g1 and T_g2 to the higher temperature with increasing the TiO$_2$ content could be attributed to the raised cross-linking density leading to a higher hindrance for the chain movement. As a result, the chain movement occurs at elevated temperature with increasing the TiO$_2$ content. For PMDA/ODA series, there is only one broad tan δ peak observed in Figure 6.5. It can be explained that the two tan δ signals merges into a broad one due to PMDA/ODA having a higher T_g than BPDA/ODA and BTDA/ODA.

Table 6.3 The glass transition temperatures (T_g) of PI/TiO$_2$ hybrid films.

TiO$_2$ Content	PMDA/ODA	BPDA/ODA		BTDA/ODA	
	T_g^b (℃)	T_g1 (℃)	T_g2 (℃)	T_g1 (℃)	T_g2 (℃)
0 wt%	368.1	276.1	-	305.4	-
1 wt%	388.3	279.3	397.5	307.5	390.1
3 wt%	429.4	313.4	411.0	312.1	414.1
5 wt%	a	322.41	412.8	327.6	415.5
7 wt%	a	350.92	414.2	342.3	416.9
9 wt%	a	a	a	363.4	419.3

[a] The hybrid film is too brittle and fragile to obtain satisfactory for measurement.
[b] The maximum in tan δ is used as the definition of glass transition temperature.

6.4 The Mechanical Properties of PI/TiO$_2$ Hybrid Films

The mechanical properties of PI/TiO$_2$ hybrid films are evaluated by DMA at both 30 ℃ and 200℃. The results of tensile stress, elongation at break and initial modulus for the hybrid films are collected in Table 6.4. The tensile stress is found to increase initially with TiO$_2$ content at 1-3 wt%. However, further addition of TiO$_2$ decreases the strength because of increasing brittleness. Values of the modulus calculated from the initial slope of the stress-strain curve shows an increase with increasing TiO$_2$ content. The modulus of these hybrid films is in the range of 2.1-4.2 GPa at 30℃. Besides, there is a more enhanced improvement in modulus at elevated temperature. On the contrary, the elongation of the hybrid films decreases with increasing TiO$_2$ content. This is presumably due to the inorganic moiety which generally has the capability of tolerating large stress but only small strain [24-25]. In addition, the series of BPDA/ODA and BTDA/ODA show larger elongation than PMDA/ODA series due to their higher flexibility. As can be seen from the above results of mechanical properties, there is considerable reinforcement for the hybrid films with small amount of TiO$_2$ incorporated.

6.5 The Thermal Stability of PI/TiO$_2$ Hybrid Films

The thermograms obtained for the PI/TiO$_2$ hybrid films under a nitrogen atmosphere at a heating rate of 20 ℃/min are shown in Figures 6.8-6.10. The decomposition temperatures (T_d), at 5 % weight loss, are given in Table 6.5. The results indicate that hybrid films start to decompose around or above 400℃ and lose 5 % weight between 490 and 590℃. Although the introduction of TiO$_2$ causes a decrease in thermal stability, all the hybrid films still reveal good thermal stability. According to the studies reported previously, the decrease in thermal stability could be attributed to the metallic compounds which can oxidatively degrade polyimide films [26-28].

Table 6.4 The mechanical properties of PI/TiO$_2$ hybrid films.

TiO$_2$ Content	Stress (MPa)[b]			Elongation (%)[c]			Modulus (GPa)[d]		
	PM	BP	BT	PM	BP	BT	PM	BP	BT
0 wt%	129.1 (70.4)	207.9 (82.4)	134.4 (77.5)	29.4 (37.8)	39.2 (55.4)	25.2 (47.3)	2.1 (1.5)	2.9 (1.5)	2.8 (1.8)
1 wt%	132.3 (73.1)	221.0 (110.7)	151.3 (79.1)	18.5 (12.2)	34.1 (51.6)	23.7 (31.5)	2.5 (1.7)	3.1 (1.7)	3.2 (1.8)
3 wt%	103.4 (59.0)	150.7 (77.1)	150.5 (86.3)	3.2 (1.7)	16.4 (14.7)	18.4 (27.9)	2.7 (1.9)	3.2 (1.9)	3.3 (2.1)
5 wt%	39.5 (21.6)	112.0 (69.6)	118.4 (48.6)	1.4 (0.7)	2.5 (7.8)	4.5 (3.2)	2.8 (2.3)	3.5 (2.3)	3.5 (2.7)
7 wt%	e	23.1 (38.2)	69.4 (45.3)	e	1.1 (1.6)	1.9 (2.3)	e	3.6 (2.4)	3.9 (3.1)
9 wt%	e	e	51.2 (42.1)	e	e	1.5 (2.1)	e	e	4.2 (3.3)

[a] PM: PMDA/ODA series; BP: BPDA/ODA series; BT: BTDA/ODA series.

[b] The first entry is corresponding to the load at break measured at 30℃; the entry in parentheses is measured at 200℃.

[c] The first entry is corresponding to the elongation at break point measured at 30℃; the entry in parentheses is measured at 200℃.

[d] The first entry is corresponding to the initial modulus measured at 30℃; the entry in parentheses is measured at 200℃.

[e] The hybrid film is too brittle and fragile to obtain satisfactory for measurement.
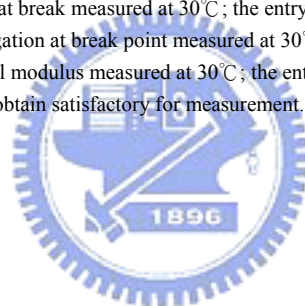
Table 6.5 The thermal decomposition temperatures (T_d) of PI/TiO$_2$ hybrid films.

TiO$_2$ Content	Decomposition temperature T_d (℃)[a]		
	PMDA/ODA	BPDA/ODA	BTDA/ODA
0 wt%	569	590	570
1 wt%	564	589	573
3 wt%	547	585	574
5 wt%	523	566	560
7 wt%	508	542	551
9 wt%	490	513	530

[a] The temperature at which 5% weight loss.

Figure 6.8 The thermogravimetric profiles of the PMDA/ODA-TiO$_2$ hybrid films.
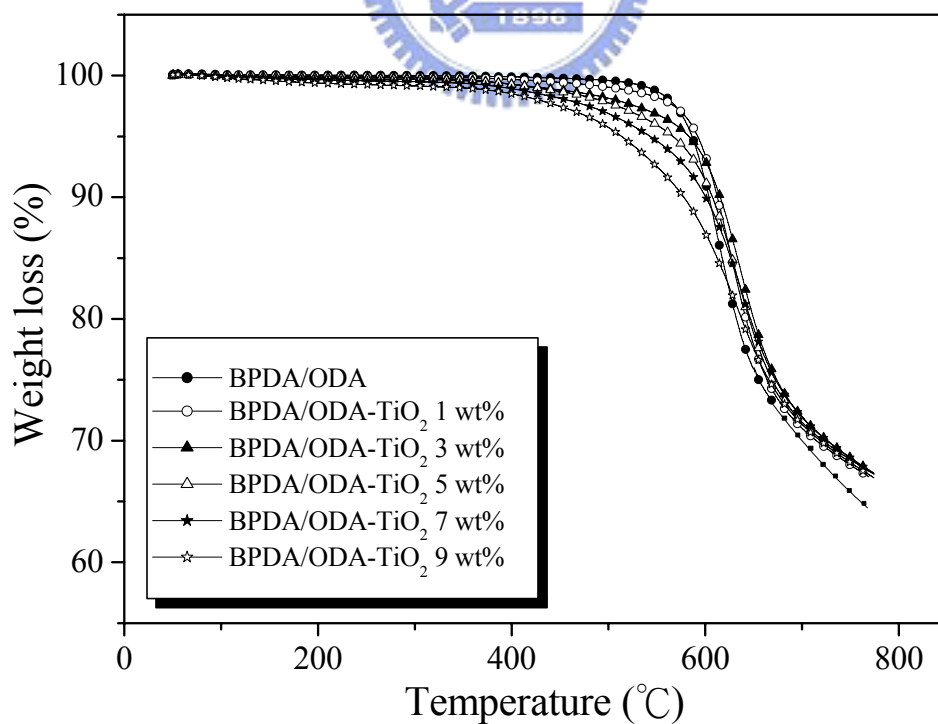
Figure 6.9 The thermogravimetric profiles of the BPDA/ODA-TiO$_2$ hybrid films.
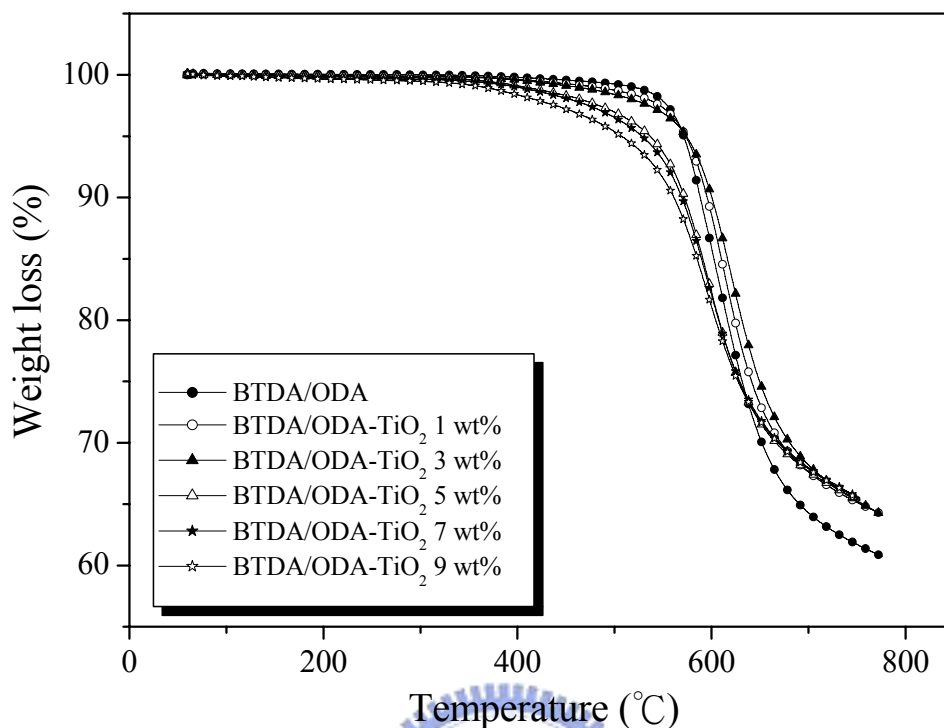
Figure 6.10 The thermogravimetric profiles of the BTDA/ODA-TiO$_2$ hybrid films.

6.6 The Electrical Properties PI/TiO$_2$ Hybrid Films

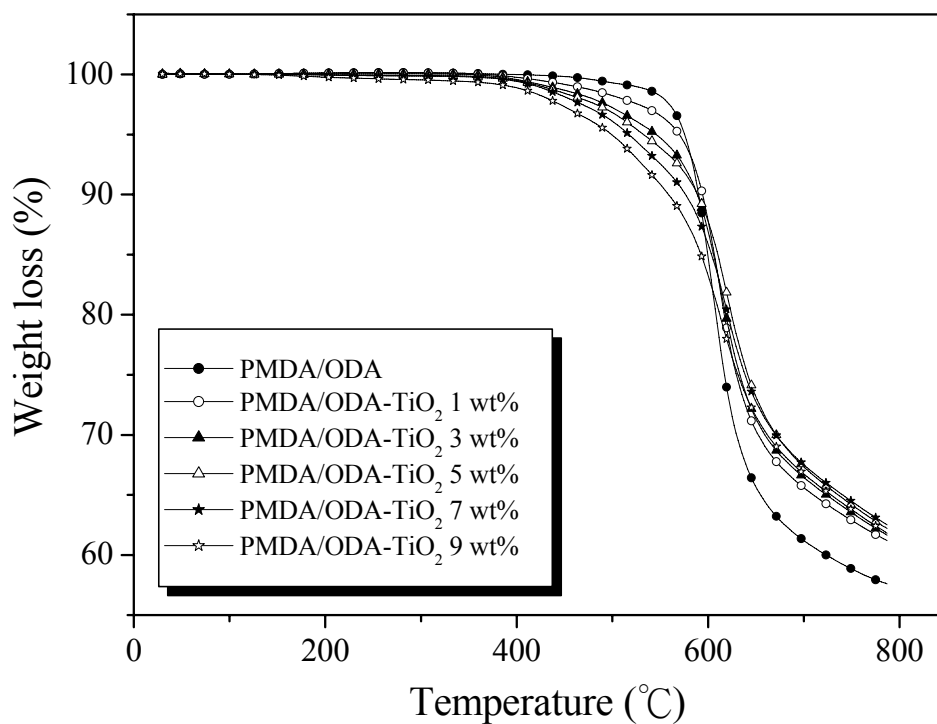The dielectric constants ($\mathbf{D}_k$) and dielectric dissipation factors ($\mathbf{D}_f$) of PI/TiO$_2$ hybrid films are measured at frequency of 1 MHz. These data are listed in Table 6.6 and Figure 6.11 is plotted as a function of TiO$_2$ content. These hybrid films have dielectric constants and dissipation factors in the range of 3.26-3.9 and 5.56-11.31, respectively. For each series of PI/TiO$_2$ hybrid films, the general trend is that the $\mathbf{D}_k$ and $\mathbf{D}_f$ increase as a function of increasing TiO$_2$ content. These results could be related to the incorporation of TiO$_2$ that can affect the water absorption, free volume, and total polarizability.

Surface resistivity ($\boldsymbol{R}_s$) and volume resistivity ($\boldsymbol{R}_v$) of PI/TiO$_2$ hybrid films are presented in Table 6.7. A trend of decreasing $\boldsymbol{R}_s$ and $\boldsymbol{R}_v$ with increasing the TiO$_2$

content is observed. It is believed that the lowered electrical surface resistivity appear to be correlative with the presence of TiO_2 on the hybrid film surface. According to Table 6.7, the electrical resistivity of the hybrid films is actually changed by introducing TiO_2. However, the effect of TiO_2 content on reducing resistivity is not so remarkable.

Table 6.6 The dielectric constants (D_k) and dielectric dissipation factors (D_f) of PI/TiO_2 hybrid films.

TiO$_2$	PMDA/ODA		BPDA/ODA		BTDA/ODA	
Content	D_k	D_f	D_k	D_f	D_k	D_f
0 wt%	3.26	7.12	3.40	5.56	3.32	6.04
1 wt%	3.42	8.13	3.43	6.37	3.34	6.05
3 wt%	3.54	8.58	3.45	6.70	3.50	6.54
5 wt%	3.66	9.29	3.53	10.33	3.62	7.15
7 wt%	3.89	10.80	3.80	10.51	3.68	7.37
9 wt%	3.96	11.31	3.90	10.76	3.74	7.69

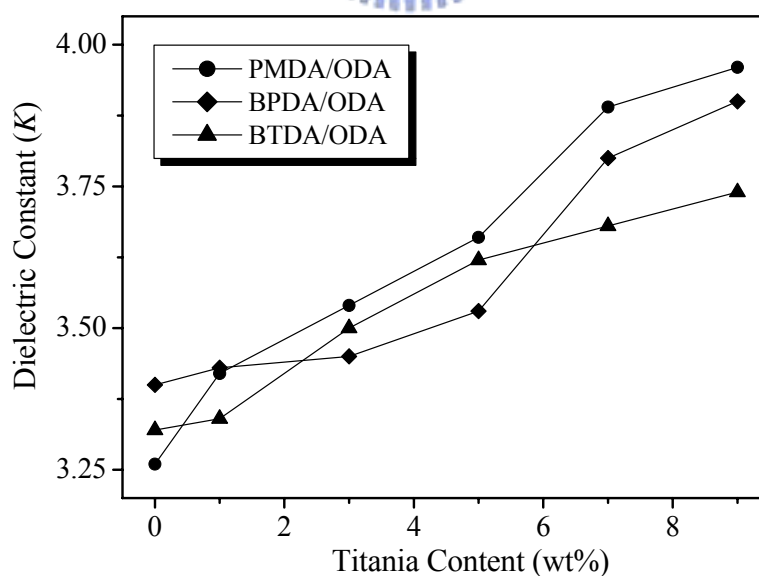[a] The dielectric constants and dielectric dissipation factors are measured at 1 MHz.

Figure 6.11 Variation of dielectric constants of the PI/TiO_2 hybrid films as a function of TiO_2 content.

Table 6.7 The surface and volume resistivities of PI/TiO$_2$ hybrid films.

TiO$_2$ Content	PMDA/ODA		BPDA/ODA		BTDA/ODA	
	R_v (Ω-cm)	R_s (Ω)	R_v (Ω-cm)	R_s (Ω)	R_v (Ω-cm)	R_s (Ω)
0 wt%	5.6×10^{16}	9.1×10^{15}	1.6×10^{17}	4.4×10^{16}	3.2×10^{17}	7.3×10^{16}
1 wt%	2.5×10^{16}	5.3×10^{15}	1.4×10^{17}	1.7×10^{16}	2.7×10^{17}	5.8×10^{16}
3 wt%	8.9×10^{15}	2.1×10^{14}	5.8×10^{16}	9.0×10^{15}	6.8×10^{16}	8.3×10^{15}
5 wt%	1.7×10^{15}	1.6×10^{14}	1.7×10^{16}	8.7×10^{15}	2.5×10^{16}	7.3×10^{15}
7 wt%	a	a	1.4×10^{16}	4.7×10^{15}	2.2×10^{16}	5.1×10^{15}
9 wt%	a	a	a	a	1.8×10^{16}	4.3×10^{15}

a The hybrid film is too brittle to be measured.

6.7 Conclusion

Three series of PI/TiO$_2$ hybrid films have been prepared via sol-gel process. The flexibility of PI/TiO$_2$ hybrid films has an order of BTDA/ODA > BPDA/ODA > PMDA/ODA. For PI/TiO$_2$ hybrid films, there is a dramatic reduction of thermal expansion as compared with host polyimide. Besides, the cross-linked structure of hybrid films reinforces the pure polyimide. The hybrid films with small amount of TiO$_2$ (1-3 wt%) are tough and has a higher tensile stress than pure polyimide. However, further addition of TiO$_2$ results in rigidity of the hybrid films that decreases the tensile stress and elongation, but increases the modulus.

According to the results of DMA studies, it points to the existence of another partially miscible inorganic/organic phase, which has a higher T_g than polyimide matrix. We are tempted to think that this phase represents the interfacial region between TiO$_2$ domains and polyimide matrix. For PMDA/ODA based hybrid films, there is only one transition at T_g because the peak related to the T_g1 is overlapped with T_g2. Observed changes in tan δ magnitude and breadth suggest that the introduction of TiO$_2$ moiety also retard the motions of the polymer chains.

Results presented herein also demonstrate that incorporating TiO_2 into polyimide did not greatly affect their thermal stability. All the hybrid films still maintain good thermal stability at temperature up to 400℃. The investigation of electrical properties suggests that reducing $\mathbf{R_s}$ and $\mathbf{R_v}$ resistivities are obtained due to the presence of TiO_2. However, the increases of dielectric constant and dissipation factor as a function of increasing TiO_2 content are observed.

6.8 Reference

1. M. H. Tsai, W. T. Whang, *J. Appl. Polym. Sci.* 81: 2500 (2001).

2. D. S. Thompson, D. W. Thompson, R. E. Southward, *Chem. Mater.* 14: 30 (2002).

3. F. Hide, K. Nito, A. Yasuda, *Thin Solid Film* 240: 157 (1994).

4. J. Wen, G. L. Wilkes, *Chem. Mater.* 8: 1667 (1996).

5. C. J. Cornelius, E. Marand, *Polymer* 43: 2385 (2002).

6. Z. Ahmad, M. I. Sarwar, S. Wang, J.E. Mark, *Polymer* 38: 4523 (1997).

7. C. J. Cornelius, E. Marand, *Polymer* 43: 2385 (2002).

8. H. L. Tyan, Y. C. Liu, K. H. Wei, *Chem. Mater.* 11: 1942 (1999).

9. C. E. Sroog, *J. Polym. Sci. Macromol. Rev.* 11: 161 (1976).

10. K. L. Mittal Eds., *Polyimide: Synthesis, Characyerization and Application*, New York (1984).

11. M. H. Tsai, W. T. Whang, *Polymer* 42: 4197 (2001).

12. M. K. Ghosh, K.L. Mittal Eds., *Polyimide, Fundamentals and Applications*, New York (1996).

13. R. J. Angelo, *U.S. Patent* 3: 785 (1959).

14. A. Clair, NASA-Langley Research Center and L. T. Taylor, *J. Appl. Polym. Sci.* 28: 2393 (1983).

15. M. M. Ellison, L. T. Taylor, *Chem. Mater.* 6: 990 (1994).

16. J. D. Rancourt, G. M. Porta, T. L. Taylor, *Thin Solid Films* 158: 189 (1988).

17. J. J. Bergmeister, L. T. Taylor, *Chem. Mater.* 4: 729 (1992).

18. S. A. Ezzell, T. A. Furtsch, E. Khor, L. T. Taylor, *J. Polym. Sci., Polym. Chem.* 21: 865 (1983).

19. M. Yoshida, N. P. Paras, *Chem. Mater.* 8: 235 (1996).

20. L. H. Sperling, *Introduction to Physical Polymer Science*, Chapter 8, Wiley (1992).

21. K. L. Mittal ed., *Polyimides: Synthesis, Characterization, and Applications*, Chapter 1-2, New York (1984).

22. M. K. Ghosh, K. L. Mittal ed., *Polyimides: Fundamentals and Applications*, Chapter 20, New York (1996).

23. D. Wilson, H. D. Stenzenberger, P. M. Hergenrother, *Polyimides*, Chapter 6, Blackie (1990).

24. B. Wang, G. L. Wilkes, J. C. Hedrick, S. C. Liptak SC, J. E. McGrath, *Macromolecules* 24: 3449 (1991).

25. P. Papadimitrakopoulos, P. Wisniecki, D. Bhagwagar, *Chem. Mater.* 9: 2928 (1997).

26. T. Sawada, S. Ando, *Chem. Mater.* 10: 3368 (1998).

27. R. K. Boggess, L. T. Taylor, *J. Polym. Sci., Polym. Chem. Ed.* 25: 685 (1987).

28. J. D. Rancourt, L. T. Taylor, *Macromolecules* 20: 790 (1987).